Electrical conductivity of $SrTi_{1-x}Ru_xO_3$

R. F. Bianchi, J. A. G. Carrió, S. L. Cuffini, Y. P. Mascarenhas, and R. M. Faria
Instituto de Física de São Carlos, Universidade de São Paulo, Caixa Postal 369, 13560-970 São Carlos, Brazil
(Received 13 January 2000)

$SrTi_{(1-x)}Ru_xO_3$ perovskite oxide compound exhibits different physical properties depending on the *x* value and the temperature range. High electrical conductivity, ferromagnetism phenomena, piezoelectricity, and superconductivity are currently properties found in this perovskite family. In this paper we present a study of electronic conduction of this mixed perovskite in function of *x* and temperature by alternating conductivity technique. Pure $SrTiO_3$ is an insulating material that progresses to a conductive one as *x* increases. The model used to explain this conductivity evolution is the random free energy barrier model developed to explain transport phenomena in disordered materials. Disorder in this perovskite is supported by diffraction studies that evidenced slight delocalizations of oxygen atoms in the lattice, added due to random substitutions of Ti^{4+} by Ru^{4+}.

I. INTRODUCTION

Studies of mixed perovskite $SrTi_{(1-x)}Ru_xO_3$ (STRO) structures have aroused considerable interest of late, since they have shown a large variety of physical effects and technological applications. $SrRuO_3$, for example, presents electrical conductivity equal to 4×10^6 $(\Omega\, m)^{-1}$ at low temperatures and 10^6 $(\Omega\, m)^{-1}$ at room temperature,[1] exhibits the rare $4d$ ferromagnetism at 160 K that is characteristic of low dimensional systems,[2] and was used as thin barrier layer with Josephson junction property in a superconductor-ferromagnetic-superconductor structure, having $YBa_2Cu_3O_{(7-x)}$ films as electrodes.[3] More recently it was also discovered that members of $Sr_{(1+x)}RuO_{(3+x)}$ systems are superconductors,[4] showing certain similarities to the high critical temperature cuprates. On the other hand, $SrTiO_3$ is a diamagnetic insulator material that presents a giant piezoelectric effect at low temperature,[5] but it acquires a semiconducting behavior when doped with iron, presenting large thermochromism[6] and electrocoloration effect.[7]

Electronic band structure of both $SrRuO_3$ cubic and orthorhombic crystalline forms were calculated by different methods showing their unambiguous metallic behavior.[8,9] Electronic conduction was also observed in $SrTiO_3$ at low temperature.[10] In this paper we show complex alternating conductivity studies of STRO structures, and that they behave as conducting disordered materials.[11,12] In such behavior, the real component of the ac conductivity $\sigma'(f)$ has a plateau at low frequencies *f*, i.e., for these frequencies the conductivity does not vary with the frequency, but above a certain frequency, denoted by critical frequency f_c, it obeys the relation $\sigma'(f)\propto f^n$, where $0\leqslant n\leqslant 1$. The imaginary component obeys a linear relation in the $\ln\sigma''(f)$vs$\ln f$ graph, in almost the whole frequency range, outlining an absorption peak at higher frequencies. Assuming that the substitution of Ru^{4+} for Ti^{4+} (or vice versa) in a STRO structure breaks the periodicity of the electric potential arrangement, we describe the complex conductivity $\sigma^*(f)$ in terms of hopping mechanism (or tunneling assisted by phonons) over electrical barriers randomly distributed in the bulk material. Delocalization of oxygen atoms in a unitary cell due to high vibration movement, observed in x-ray diffraction studies, also contributes to such aleatory barrier distribution.

II. EXPERIMENT

Solid solutions of STRO were prepared by mixing Sr and Ti in a 1:(1-*x*) ratio obtained in water solution with appropriate stoichiometric amounts of $TiCl_4$ and $Sr(NO_3)_2$. A solution containing $(NH_4)_2CO_3$ and NH_4OH was then slowly added and the final mixture stirred until the complete precipitation of the solid $SrTiO_3$. After that, the product was filtered, washed in water, dried at 120 °C, and kept at 1100 °C for 3 h. Afterwards the solid solution of STRO was prepared adding a molar amount *x* of RuO_2 and the mixture was ground until a fine powder was obtained. The final mixture was then heated again at 1100 °C for 3 h.

Powder diffraction patterns of STRO solid solutions ($x=0.01$, 0.05, 0.10, 0.20, and 0.33) were obtained by a rotating anode Rigaku Denki diffractometer, in 0.02° steps, with a counting time of 5 s, over the range $10^0\leqslant 2\theta\leqslant 120^0$. The structures were refined by the Rietveld method using the DBWS and GSAS programs, until the acceptable discrepancy factors of 5%, 10%, 15%, and 3%, respectively, for R-Bragg, Rp, Rwp, and S were reached. The results are in agreement with recent $SrRuO_3$ crystal structure determination carried out by the powder neutron diffraction method.[13]

Impedance measurements were carried out using a frequency response analyzer controlled by a programmed software, operating in the $10–10^6$ Hz frequency range. The measurements were performed at different temperatures, between 100 and 300 K under high vacuum.

III. RESULTS

X-ray diffraction for different *x* values showed three crystallographic space groups: $Pm\bar{3}m$ for *x* below 0.30, $I4/mcm$ for $0.30<x<0.40$, and $Pnma$ for *x* above 0.40.[13] The refinement of the x-ray patterns by the Rietveld method discarded

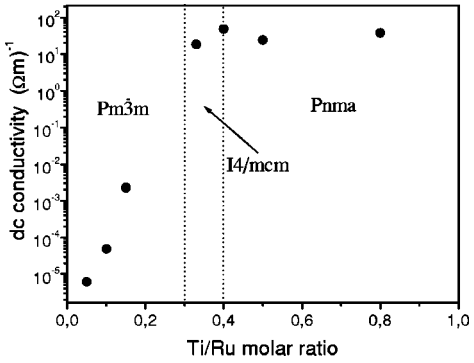

FIG. 1. dc conductivity of $SrTi_{(1-x)}Ru_xO_3$ for different x values: 0.01, 0.05, 0.10, 0.15, 0.33, 0.40, 0.50, and 0.80. Measurements carried out at 300 K under vacuum.

any other primitive unit cell different from that of $Pm\bar{3}m$. In case of an ordered Ti^{4+} for Ru^{4+} substitution, the cubic face centered $Fm\bar{3}m$ should be observed. Then, to keep the $Pm\bar{3}m$ structure, a spatially random substitution of Ti by Ru must occur. Furthermore, high values of thermal vibration factors obtained for the oxygen atoms, by the Rietveld refinement, indicate a disorder in the location of these atoms in the STRO structure. High thermal vibration factors are observed even at low temperatures as shown in the detailed analysis carried out with $SrTi_{0.90}Ru_{0.10}O_3$ at 160 K.[13] The large thermal anisotropic displacement of O_2 in the $SrRuO_3$ structure was also evidenced by neutron diffraction experiments.[14]

Figure 1 shows the dc conductivity σ_{dc} in function of x which measures the amount of replacement of Ti by Ru in the unit cell of STRO. One may observe that for $x<0.30$, the conductivity increases linearly with x, that is the range in which STRO exhibits $Pm\bar{3}m$ symmetry. Above this value, i.e., for $x>0.30$, the conductivity remains practically constant, and the structure changes from $Pm\bar{3}m$ to $I4/mcm$ at $x=0.30$, and from $I4/mcm$ to $Pnma$ at $x=0.40$. Complex conductivity measurements carried out with samples of STRO with $x>0.15$ showed that the real part of ac conductivity $\sigma'(f)$ is frequency independent in the whole range of 10 Hz to 1 MHz whose value was approximately equal to 30 $(\Omega\, m)^{-1}$ (results not shown) coincident, therefore, to that measured by dc technique (Fig. 1). However, for STRO samples with x lower than 0.15, $\sigma'(f)$ presents a frequency-independent part at low frequencies, the dc conductivity (σ_{dc}) plateau, followed by a part in which the conductivity obeys approximately the $\sigma'(f)\propto f^n$ relation. The frontier between these two regions in the $\sigma'(f)$ curve is not well defined but is determined by a critical frequency f_c. Another

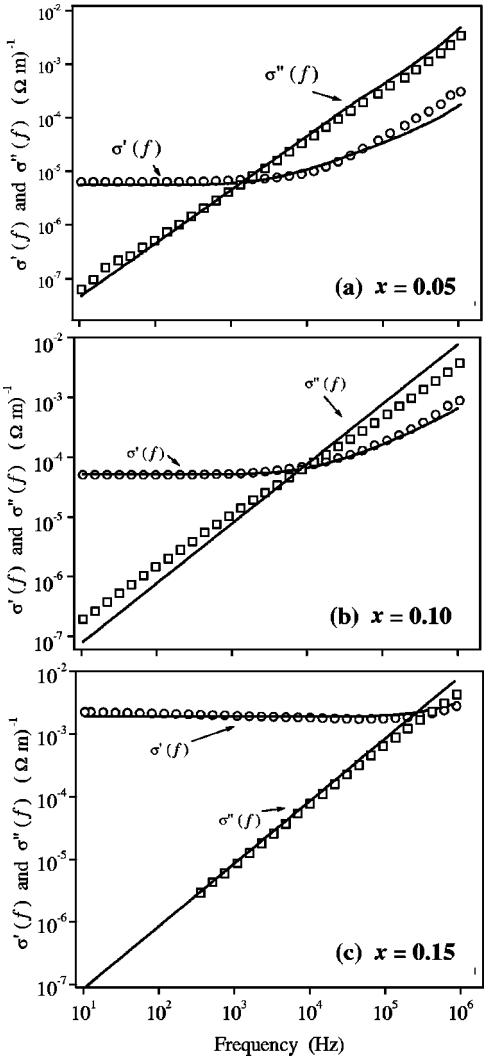

FIG. 2. $\sigma'(f)$ and $\sigma''(f)$ components of the complex conductivity. (a) $SrTi_{0.95}Ru_{0.05}O_3$, (b) $SrTi_{0.90}Ru_{0.10}O_3$, and (c) $SrTi_{0.85}Ru_{0.15}O_3$. Measurements carried out at 300 K under vacuum. Full lines represent the theoretical fittings.

characteristic of the $\sigma'(f)$ curve is that the low-frequency plateau is shorter (i.e., f_c is small); the sample is less conductive, which for STRO means the x value is smaller (see Fig. 2). The imaginary component of the conductivity $\sigma''(f)$ presents a quasilinear behavior in the double-logarithm scale, irrespective the x value; this, probably is part of an absorption curve whose maximum should be reached in a frequency beyond the scope of present measurements. The intersection between $\sigma'(f)$ and $\sigma''(f)$ curves is used as a method of approximately finding the critical frequency f_c. Experimental values of σ_{dc} and f_c obtained from measurements carried

TABLE I. Data of fittings between Eq. (1) and experimental results for $SrTi_{0.95}Ru_{0.05}O_3$, $SrTi_{0.90}Ru_{0.10}O_3$, and $SrTi_{0.85}Ru_{0.15}O_3$ samples at 300 K under vacuum.

Samples	σ_{dc} $(\Omega\ \mathrm{m})^{-1}$	σ_0 $(\Omega\ \mathrm{m})^{-1}$	K	γ'_{min} (Hz)	σ_0/γ'_{min} $(\Omega\ \mathrm{mHz})^{-1}$
$SrTi_{0.95}Ru_{0.05}O_3$	6.2×10^{-6}	5.7×10^{-6}	50	1.1×10^{3}	5.3×10^{-9}
$SrTi_{0.90}Ru_{0.10}O_3$	4.9×10^{-5}	4.8×10^{-5}	65	3.5×10^{3}	1.4×10^{-8}
$SrTi_{0.85}Ru_{0.15}O_3$	2.3×10^{-3}	1.9×10^{-3}	75	1.9×10^{5}	1.0×10^{-8}

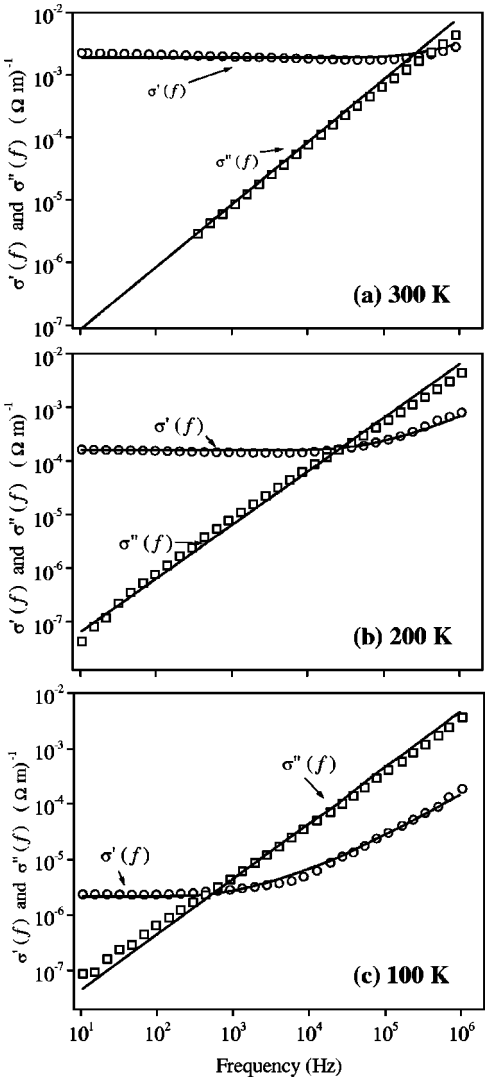

FIG. 3. $\sigma'(f)$ and $\sigma''(f)$ components of the complex conductivity of $SrTi_{0.85}Ru_{0.15}O_3$. (a) 300 K, (b) 200 K, and (c) 100 K. Measurements carried out under vacuum. Full lines represent the theoretical fittings.

out with samples of x equal to 0.05, 0.10, and 0.15 are shown in Table I; the angular coefficient n is approximately 0.7.

Figure 3 shows measurements of both $\sigma'(f)$ and $\sigma''(f)$ carried out with the sample of $x=0.15$, for several temperatures: 100, 200, and 300 K. The conductivity σ_{dc} decreases from 2.3×10^{-3} $(\Omega\, m)^{-1}$ at 300 K to 2.5×10^{-6} $(\Omega\, m)^{-1}$ at 100 K, while f_c becomes higher as the conductivity of the material increases, i.e., as the temperature increases. Table II shows experimental values of σ_{dc} and adjusted values of σ_0, γ'_{min}, and K. However, it is important to note that σ_{dc} is close to σ_0 and γ'_{min} is close to f_c. The exponent n is slightly smaller than 0.7, as obtained from measurements at 150 and 100 K. On the other hand, $\sigma''(f)$, which is always a quasilinear function in the double-logarithm scale, practically does not vary with the temperature.

IV. THEORETICAL CONSIDERATIONS

Electronic conduction behavior of isotropic-disordered media depends strongly on their bulk structural irregularities. A random distribution of energy barriers, among the electronic energy levels, is derived from such irregularities. In a STRO structure with x different from 0 and 1, x determining the Ru amount in STRO, it is reasonable to assume a break in the regular potential arrangement of the crystal. Furthermore, the high vibration of oxygen atoms also generates distortions on the local potential, contributing to the disarrangement of the potential in the crystal network. In such a picture, the electronic conduction may occur, at least partially, via hopping, or via phonon assisted tunneling, among localized states, whose transition rate depends on the spatial distance and/or the energy difference of the localized energy levels. In the concept of hopping conduction, all the information about the disorder is comprised in the hopping time distribution function $\Psi(t)$. For a disordered solid this function is determined by hopping over a random distributed energy barrier, as proposed by Dyre.[15] From the continuous time random walk approach applied to a regular lattice, and obeying the Kubo's fluctuation theorem, Odagaki and Lax[16] derived the efficacious expression for the complex conductivity $\sigma^*(\omega)=C[1/\phi^*(i\omega)-i\omega]$, where $\phi^*(i\omega)$ is the Laplace transform of $\phi(t)$ that is the probability residence for a time t in a given site (localized energy level), and C is a constant that depends on the carrier density. $\phi(t)$ is related to the hopping time distribution function by $\Psi(t)=-d\phi(t)/dt$.

For each site i, one may associate a residence time function $\phi(t)=\exp(-\gamma_i t)$ that represents an exponential decay, where γ_i is a frequency escape parameter that obeys an Arrhenius processes, $\gamma_i=\gamma_0 e^{-W_i/kT}$; where γ_0 is a frequency factor and W_i is the barrier energy of site i, The function $\Phi(t)=\langle\phi(t)\rangle$ is then defined as the average of all possible aleatory exponential decay processes. From the general expression derived by Odagaki and Lax and the concepts exposed above we easily derived the Dyre expression for the

TABLE II. Data of fittings between Eq. (1) and experimental results for $SrTi_{0.85}Ru_{0.15}O_3$ sample at different temperatures under vacuum.

Temperature (K)	σ_{dc} $(\Omega\ m)^{-1}$	σ_0 $(\Omega\ m)^{-1}$	K	γ'_{min} (Hz)	σ_0/γ'_{min} $(\Omega\ mHz)^{-1}$
300	2.3×10^{-3}	1.9×10^{-3}	75	1.9×10^{5}	1.0×10^{-8}
250	6.6×10^{-4}	5.5×10^{-4}	72	7.0×10^{4}	7.9×10^{-9}
200	1.6×10^{-4}	1.6×10^{-4}	71	2.1×10^{4}	7.4×10^{-9}
150	3.4×10^{-5}	3.2×10^{-5}	70	4.5×10^{3}	7.1×10^{-9}
100	2.3×10^{-6}	2.1×10^{-6}	62	3.5×10^{2}	6.0×10^{-9}

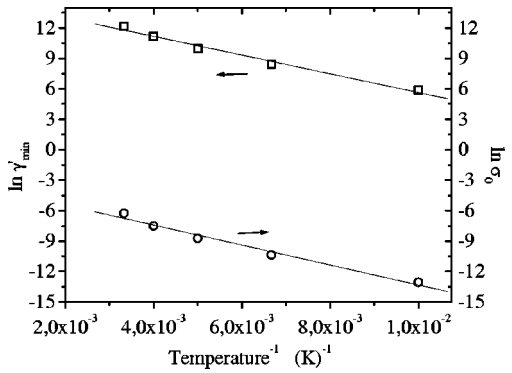

FIG. 4. $\ln \gamma'_{min}$ vs T^{-1} (□) and $\ln \sigma_0$ vs T^{-1} (○) from data of Table II. Both curves present an activation energy $E_a = 0.085$ eV when fitted by the Arrhenius process.

complex conductivity,[17] for the case where γ_{min}, associated to W_{max}, is much smaller than γ_{max}, associated to W_{min}:

$$\sigma^*(\omega) = \sigma_0 \left[\frac{i\omega/\gamma_{min}}{\ln(1 + i\omega/\gamma_{min})} \right] + i\omega\epsilon'. \tag{1}$$

This derivation assumes a continuous distribution between the lowest W_{min} and the highest W_{max} energy barrier values. The value $\sigma_0 (= C\gamma_{min} \ln\lambda)$ is obtained taking into account the limit $\omega \to 0$, where $\lambda = \gamma_{max}/\gamma_{min}$. The additional term $i\omega\epsilon'$ comes from the dielectric response of the material. $\epsilon' = K\epsilon_0$, where K is the dielectric constant and ϵ_0 is the vacuum permissivity.

V. PARAMETERS OF THE MODEL

Considering that there are irregularities in the STRO structure, due to the oxygen delocalization and the aleatory Ru^{4+}-Ti^{4+} substitution, its potential landscape is such that a carrier in movement under an applied field should overcome potential barriers randomly distributed in position and in energy in the bulk's material. This may occur via hopping, overleaping the barriers, or by tunneling via phonons assistance. In this picture the model of an energy barrier randomly distributed in a system, succinctly described above and expressed by Eq. (1), seems to be a good approach in describing the complex conductivity shown in Figs. 2 and 3. Equation (1) also has a contribution of the dielectric relaxation to the conductivity of the material. Continuous curves of all graphs of Figs. 2 and 3 are the fitting obtained by Eq. (1). In this expression γ_{min} is the frequency escape of higher energy barrier W_{max} and $\gamma'_{min} = 2\pi\gamma_{min}$ is one of the adjust parameter, having a value close to f_c. The other adjusted parameters are the σ_0, whose value is close to σ_{dc}, and the dielectric constant K. All adjusted values are shown in Tables I and II. Both σ_0 and γ'_{min} increase with Ru content and temperature, and the ratio σ_0/γ'_{min} varies only slightly with the temperature, as shown in Table II. This is in agreement with the expression $\sigma_0/\gamma'_{min} = C' \ln\lambda$, where $\lambda = \gamma_{max}/\gamma_{min}$. Indeed in Fig. 4 the curves show that monolog curves $\ln\sigma_0$ and $\ln\gamma'_{min}$ vs the temperature reciprocal are parallels showing and Arrhenius process and having, therefore, the same activation energy $E_a = 0.085$ eV. This activation energy is a reasonable value for carrier traps. The dielectric constant K increased slightly with the material conductivity, i.e., it was bigger for higher x or temperature. However, a more accurate study should take into account its dependence with the frequency.

VI. CONCLUSIONS

Since the remarkable paper of Pollak and Geballe about the effect of *n*-type doping in crystalline silicon,[18] in which a power-law frequency dependence $\sigma'(f) \propto f^n$ of the real part of the conductivity was observed, similar ac conductivity behavior has been observed in a great variety of disordered solids. Several studies based on hopping conductivity (electronic, polaronic or even ionic) have been developed, but some disagreements with experimental results were always present (for a brief review see Ref. 12). Treatments of hopping in a manifold of states near the Fermi level results in a weak temperature-dependent ac conductivity. The classical approach of pair approximation,[19] predicted that the power-law exponent n has a value to 0.8, the dc conductivity varied strongly with temperature. This strong temperature dependence can be explained in terms of thermal activation of charge carriers from localized states in the gap to the mobility edge.[20] Such localized states being generated or by both phenomena: distortion in a pure lattice (pure lattice defined by $x = 1$ or $x = 0$) caused by changing Ti for Ru, and delocalization of oxygen atoms in a primitive cell. The σ_{dc} or σ_0 would then be proportional to $\exp(-E_a/KT)$ with E_a being the activation energy. The random free-barrier approach[15,17] proved to be a good model for STRO structures not only because it fit the ac conductivity results well but mainly because the results showed the same activation process for both σ_0 and γ'_{min} as foreseen by this model. It is important to remark that the dielectric constant K showed weak variation with the frequency and temperature.

ACKNOWLEDGMENTS

This work was sponsored by Fapesp and CNPq.

[1] F. Fukunaga and N. Tsuda, J. Phys. Soc. Jpn. **63**, 3798 (1994).
[2] D.J. Singh, J. Appl. Phys. **79**, 4818 (1996).
[3] L. Antognazza, K. Char, T.H. Geballe, L.L.H. King, and A.W. Sleight, Appl. Phys. Lett. **63**, 1005 (1993).
[4] Y. Meno, H. Hashimoto, K. Yoshida, S. Nishizaki, T. Fujita, J.G. Bednorz, and E. Lichtenberg, Nature (London) **372**, 532 (1994).
[5] D.E. Grupp and A.M. Goldman, Science **276**, 392 (1997).
[6] R.L. Wild, E.M. Rockar, and J.C. Smith, Phys. Rev. B **8**, 3828 (1973).
[7] J. Blanck and D. Staebler, Phys. Rev. B **4**, 3548 (1971).
[8] G. Santi and T. Jarlborg, J. Phys.: Condens. Matter **9**, 9563 (1997).
[9] P.B. Allen, H. Berger, O. Chauvet, L. Forro, T. Jarlborg, A. Junod, B. Revaz, and G. Santi, Phys. Rev. B **53**, 4393 (1996).
[10] C. Lee, J. Yashia, and J.L. Brebner, Phys. Rev. B **3**, 2525 (1971).
[11] K. Jonsher, Nature (London) **267**, 673 (1977).

[12] G.A. Niklasson, J. Appl. Phys. **66**, 4350 (1989).
[13] J. A. G. Carrió, Ph.D. thesis, Institute of Physics of São Carlos/USP, Brazil 1998.
[14] B.J. Kennedy and B.H. Hunter, Phys. Rev. B **58**, 653 (1998).
[15] J.C. Dyre, J. Appl. Phys. **64**, 2456 (1988).
[16] T. Odagaki and M. Lax, Phys. Rev. B **24**, 5284 (1981).
[17] R.F. Bianchi, G.F. Leal Ferreira, C.M. Lepienski, and R.M. Faria, J. Chem. Phys. **110**, 4602 (1999).
[18] M. Pollak and T.H. Geballe, Phys. Rev. **122**, 1742 (1961).
[19] I.G. Austin and N.F. Mott, Adv. Phys. **18**, 41 (1969).
[20] E.A. Davis and N.F. Mott, Philos. Mag. **22**, 903 (1970).